

Mid to High-Frequency Ambient Noise Anisotropy and Notch-Filling Mechanisms

Patrick Ferat & Juan Arvelo

Johns Hopkins University Applied Physics Laboratory, 11100 Johns Hopkins Rd., Laurel, MD 20723-6099

Abstract Mid to high-frequency (1-20 kHz) noise is generally dominated by wind-driven wave activity but under certain conditions potentially exploitable ambient noise fields can be severely degraded by nearby ships, especially in the lower end of the band. The use of directive elements and adaptive methods are shown as possible ways to mitigate this problem. For a submerged receiver in a downward-refracting environment without nearby ships, a vertical noise notch that can offer increased array gain over the directivity index can be filled in by scattering from volume inhomogeneities. Just outside the notch, the ambient noise vertical directivity is sensitive to the assumed surface source directionality. A ray-based model is used to assess the sensitivity of the performance of a vertical line array and a volumetric array to these mechanisms in a tactically relevant environment.

INTRODUCTION

An understanding of the physics of ambient noise generation in the mid to high-frequencies is required in order to assess the capabilities of underwater acoustic systems that operate in that band. Some typical applicable systems are underwater communications, tomography and both active and passive sonar. For example, one way to mitigate passive (or active) sonar clutter due to distant shipping in bearing time recorder (BTR) displays is to operate at higher frequencies. In addition, higher frequency systems are attractive because of the reduced size and greater portability promised by high frequency arrays. A brief review of past ambient noise work is given first, followed by a description of current model developments.

Underwater acoustic ambient noise contains a surface-generated anisotropic component that is typically dominant over the isotropic thermal noise [1]. The ubiquitous thermal noise is due to molecular agitation and represents an absolute minimum level independent of sea conditions. At high frequencies, the surface generated component consists mainly of wind-driven (collapsing bubbles) noise with occasional shipping and biologic contributions. The theoretical study in [1] assumed straight-line propagation of rays and estimated the spatial correlation for monopole and dipole point sources.

A few years later Liggett and Jacobson [2] used a ray-based approach under idealized environmental conditions to compare source element directionality on estimated correlation function between vertically spaced point receivers. Two decades later Kuperman and Ingenito [3] developed a normal-mode approach for a stratified ocean, but their solution implies the use of a single layer of monopole point sources. Hamson [4] modified Kuperman and Ingenito's approach to model point sources with general vertical directivity to determine the effects of environmental parameters and source directionality on the noise level and the array response.

An accurate simulation of the performance of a passive sonar system requires an equally accurate estimation of the ambient noise. Since ambient noise is not isotropic, arrays with vertical aperture may be capable of harnessing additional gain (when steering towards the horizontal or below) over what it would otherwise have under isotropic conditions.

Wind-generated ambient noise is generally highest at elevation angles looking towards the sea surface and lower at angles towards the ocean floor. The difference in levels between the positive and negative elevation angles is a manifestation of the bottom loss at dominant grazing angles (when including corrections to account for refraction and attenuation). The oceanic waveguide's multipath effect and downward-refractive sound speed profile cause near horizontal ambient noise to be very low. This noise notch may be filled by the isotropic component of the ambient noise. Aredov [5], for example, hypothesizes an isotropic floor mechanism due to volume scattering. However, there is no known experiment that has been able to confirm this possible notch-filling mechanism.

Kennedy and Szlyk [6] collected ambient noise on two ten-wavelengths (16 & 32 kHz) vertical arrays off the Bahamas for a one-year interval. They were able to collect samples at various wind speeds, but only the broadside beam data were available. Despite the limitation of their measurement, they were able to show a distinct difference in the noise statistics that appear to correlate with the presence or absence of whitecaps. They found that their noise model requires dipole sources when whitecaps (high sea states) are present and a layer of monopole sources in their absence (low sea states). In this paper, the reference to the Kennedy model applies to the former.

Harrison [7] justified the use of a simple ray-based approach for high-frequency wind-driven noise modeling by demonstrating similar coherence function in a range-independent waveguide to that obtained with a normal-mode approach. He later extended the ray-based approach to account for range-dependent environments [8]. An analytic model similar to that of Harrison is used model wind-driven noise limited by a volume scattering component. An efficient ray-based computational model is described to include a shipping noise component. The resulting simulation tool is used here to estimate mid to high-frequency passive array performance in the presence of nearby shipping noise in addition to the wind-driven component.

THEORY

The noise model developed by the Johns Hopkins University Applied Physics Laboratory (JHU/APL) is a hybrid model that has made use of published models and theories obtained in the literature. The calculation of the vertical noise directivity is based on [7], but modified to allow for arbitrary surface source directionality [6] and also includes a volume scattering mechanism [5]. Once the ambient noise directionality is obtained, we calculate a Cross Spectral Density (CSD) matrix for an array of elements, as described by [7,9]. The CSD for shipping is separately calculated by incoherently summing the CSD matrices of individual ships. For a particular environment, ship locations and speeds (i.e., source level) are described by a realization of the Historical Temporal Shipping (HITS). In the present model, ships are stationary and the

bathymetry is range-independent. The following sections provide additional detail on each of these sub models.

Wind-Generated Ambient Vertical Noise Directivity

Wind-generated ambient noise is assumed to be azimuthally isotropic but anisotropic in vertical. The anisotropy in the vertical is due primarily by the sound speed profile, the bottom loss and the depth of the receiver. We ignore any azimuthal or range dependence in bathymetry, wind speed, bottom composition and sound speed in the water column. Therefore, the model is applicable for predicting the noise field from noise sources that are relatively close to the receiver. In addition, the model does not account for any temporal fluctuations of the sound speed typical of internal waves which can have a substantial effect on propagation in certain environments.

The following ambient noise spatial coherence equation was derived in [7]:

$$\mathbf{r}(d, \mathbf{g}) = 2\mathbf{p} \int_0^{p/2} \frac{e^{ikd \sin(\mathbf{f}_r) \sin(\mathbf{g})} e^{-as_p} + R_b e^{-ikd \sin(\mathbf{f}_r) \sin(\mathbf{g})} e^{-a(s_c - s_p)}}{[1 - R_s R_b e^{-as_c}]} \times$$

$$J_o(kd \cos \mathbf{f}_r \cos \mathbf{g}) \sin^{2m-1} \mathbf{f}_s \cos \mathbf{f}_r d\mathbf{f}_r \quad (1)$$

where k is the wavenumber, d is the element separation, \mathbf{g} is the element pair orientation, \mathbf{f}_r is the vertical angle at the receiver measured from the horizontal, \mathbf{f}_s the vertical angle of the surface source measured from the horizontal, $2m-1$ is the surface source directivity exponent of the sine function, R_s and R_b are the surface and bottom plane-wave reflection coefficients, respectively. The exponential terms containing a are absorption losses for the ray paths s_c and s_p .

When the receiver separation $d=0$ (and $\gamma=0$), the spatial coherence is equivalent to the omni noise power. Assuming dipole sources ($m=1$), negligible absorption and surface losses, Eq. (1) can be simplified to give the element omni power N :

$$N = 2\mathbf{p} \int_0^{p/2} \frac{1 + R_b}{[1 - R_b]} \sin(\mathbf{f}_s) \cos(\mathbf{f}_r) d\mathbf{f}_r$$

$$= 2\mathbf{p} \int_0^{p/2} \frac{1}{[1 - R_b]} \sin(\mathbf{f}_s) \cos(\mathbf{f}_r) d\mathbf{f}_r + 2\mathbf{p} \int_0^{p/2} \frac{R_b}{[1 - R_b]} \sin(\mathbf{f}_s) \cos(\mathbf{f}_r) d\mathbf{f}_r \quad (2)$$

The first integral term represents the noise contribution coming from above the receiver where the integrand contains the Vertical Noise Directionality (VND) function $\frac{\sin(\mathbf{f}_s)}{1 - R_b}$ and the solid angle component $\cos(\mathbf{f})d\mathbf{f}$. The second integral represents the noise contribution from below the receiver, where the integrand VND component is $R_b \frac{\sin(\mathbf{f}_s)}{1 - R_b}$, simply the upward directivity scaled by the bottom loss.

In a hypothetical deep water iso-speed environment $q_s \sim q_r$ and the second integral term vanishes when $R_b \ll 1$ (e.g., large bottom loss). When applying the dipole surface source strength A [12] Eq. (2) simplifies to:

$$N_{deep\ water} = 2pA \int_0^{p/2} \sin(\mathbf{f}_r) \cos(\mathbf{f}_r) d\mathbf{f}_r = pA \quad (3)$$

The evaluation of Eq. (3) represents the omni power in a deep water, high bottom loss and iso-speed environment. This result is identical to Eq. (55) in [12] which was derived from equations based on a different noise model than shown here.

The derivation shown in Eq. (3) could be re-derived for different values of m , but the integral may not be as simple to evaluate analytically as it is for the case of dipole surface sources. Although convenient, the surface directionality function need not be described via simple trigonometric functions like $\sin^n(\mathbf{f}_s)$, but rather it may be represented by the general function $D(\mathbf{f}_s)$. Since A is applicable to dipole surface sources, a scaling factor is applied to insure that the deep water, iso-speed omni power due to any arbitrary source directivity function $D(\mathbf{f}_s)$ is identical to that obtained by Eq.(3). In the following expressions, A_s represents the effective arbitrary surface source level which also includes the 2π term.

The JHU/APL model can also describe the surface noise source directionality proposed by Kennedy [6], which is most sensitive to whether or not white caps are present. In the absence of white caps, an effective source directivity function is modeled by incoherently summing the contribution of monopole source layers below the surface. With white caps present, the source directionality is described by dipoles. Kennedy acknowledges that under whitecap conditions, sub-surface monopole sources are present but suggests that the wave crashing and spray events are more dominant.

Therefore, the general expression for VND becomes (negative angles looking up):

$$VND(\mathbf{f}_r^-) = \frac{A_s \cdot l_D \cdot D(\mathbf{f}_s)}{\sin \mathbf{f}_s \cdot (1 - R_s(\mathbf{f}) \cdot R_b(\mathbf{f}) \cdot l_C)}$$

and,

$$VND(\mathbf{f}_r^+) = R_b(\mathbf{f}) \cdot l_{DC} \cdot VND(\mathbf{f}_r^-) \quad (4)$$

where A_s is the scaled surface source strength applicable to an arbitrary surface source directivity D . The terms l_D , l_C and l_{DC} represent the absorptive losses of the surface to receiver ray, the ray path cycle distance and the difference path, respectively.

A volume scattering mechanism is implemented to limit the level of the noise at low elevation angles [5]. The model assumes that each elemental volume in the water column scatters noise omni-directionally. The incident power is the omni noise power (assumed to be depth independent) and the volume scattering strength is assumed to be depth-independent. The contribution of distant volume scatterers is limited by absorption. Currently, the volume scattering strength can be user input or selected from average values listed in [12].

An example of the sensitivity of the VND model to surface directionality is shown in Fig. 1. The sound speed profile (GDEM, [13]), bottom loss [12], volume scattering strength of -72 dB and wind speed (5 m/s) are typical of the summer conditions in the Strait of Hormuz (25° 48 N, 56° 48 E). The VND assuming dipole surface sources are

shown in (a) and VND using Kennedy's monopole surface directionality model for low wind speeds (e.g., model of a depth distribution of monopole sources when white caps are absent at low wind speed) are shown in (b), negative elevations look up to the surface. Sub-plots (c) and (d) show the sound speed and bottom loss. Of note are the significant differences in the shape of VND for angles outside the notch.

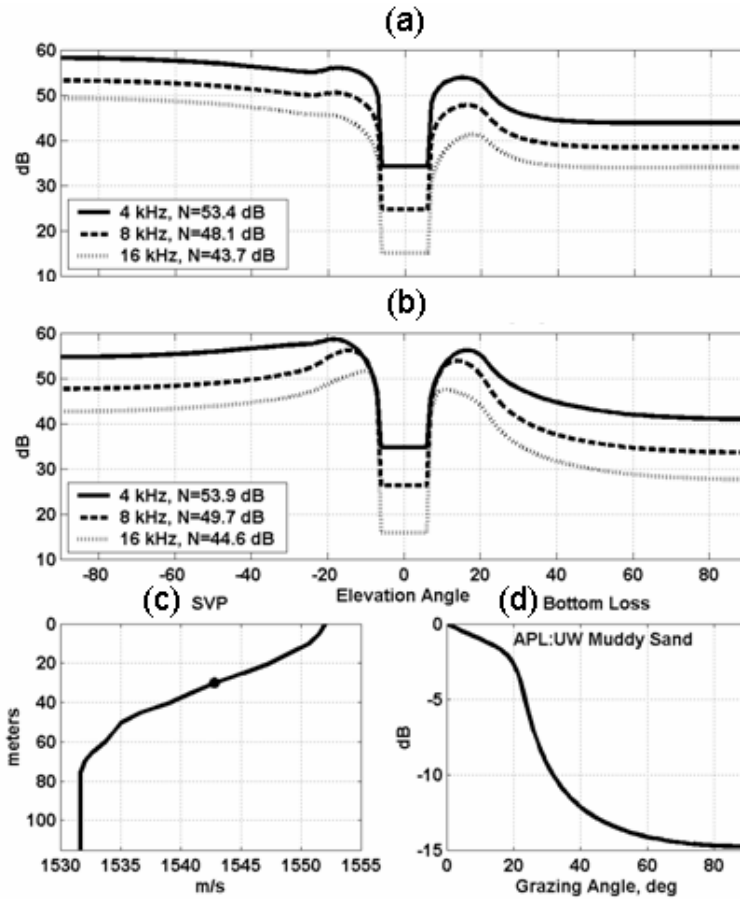


FIGURE 1. Ambient vertical noise directionality in Strait of Hormuz for receiver at 30 m 5 m/s wind speed and VSS=-72 dB, (a) dipole surface source directionality, (b) Kennedy surface source directionality, (c) sound speed profile and (d) bottom loss versus grazing angle

Via [9,10], VND can be mapped to a CSD matrix for an arbitrary array of elements. The implementation is straightforward and is not repeated here.

Cross Spectral Density of Shipping Noise

The CSD of shipping noise is determined by the incoherent sum of the CSD of all ships. The ray-based model CASS/GRAB [13] provides the eigenray launch, arrival angles and transmission loss versus range for a source at 5 meters. The same environmental inputs used for the noise (SVP, interface losses, etc) are used to maintain consistency between the ambient noise and shipping models. A separate module generates a shipping realization of the HITS database [13], for a given season/month and

location. This realization provides the location (azimuth and range) of each ship and also specifies the ship type and speed. A source level is associated with ship type and speed based on [14]. A shipping realization in the Straits of Hormuz overlays unclassified bathymetry, Fig. 2.

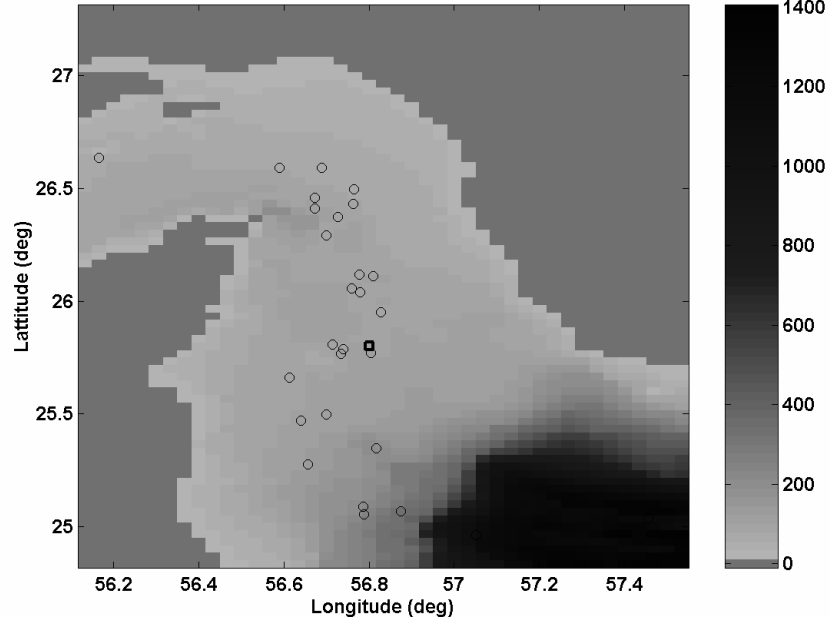


FIGURE 2. Bathymetry (in meters) and a shipping realization in the Straits of Hormuz. The circles represent ships and the square represents the location of the receiver arrays.

For a ship at a given range, consider that there are M eigenrays to the center element of an array of N elements. Letting p be the complex pressure matrix of size $N \times M$, each element of this matrix p is evaluated for element n and ray m as:

$$p_n^m = a_m \cdot \exp(i(k_x^m x_n + k_y^m y_n + k_z^m z_n)) \quad (5)$$

where a_m represents the received level pressure amplitude, and the terms in the exponential are the plane-wave arrival vectors for each element position for the given ray m . Ignoring any multi-path interference, the CSD matrix for a single ship s is simply:

$$R_{SHIP(s)} = p p' \quad (6)$$

and the total CSD matrix for all ships is:

$$R_S = \sum_{s=1}^{\infty} R_{SHIP(s)} \quad (7)$$

RESULTS

Consider two co-located receiver arrays located at a position represented by the square in Fig. 2. The first array is a 3-plane 72 element volumetric array with 10 kHz design frequency in a plane, but with a 0.8λ plane separation. The second array is a 16 element Vertical Line Array (VLA) with a design frequency of 10 kHz. The element positions and corresponding beam patterns at 8 kHz are shown in Fig. 3.

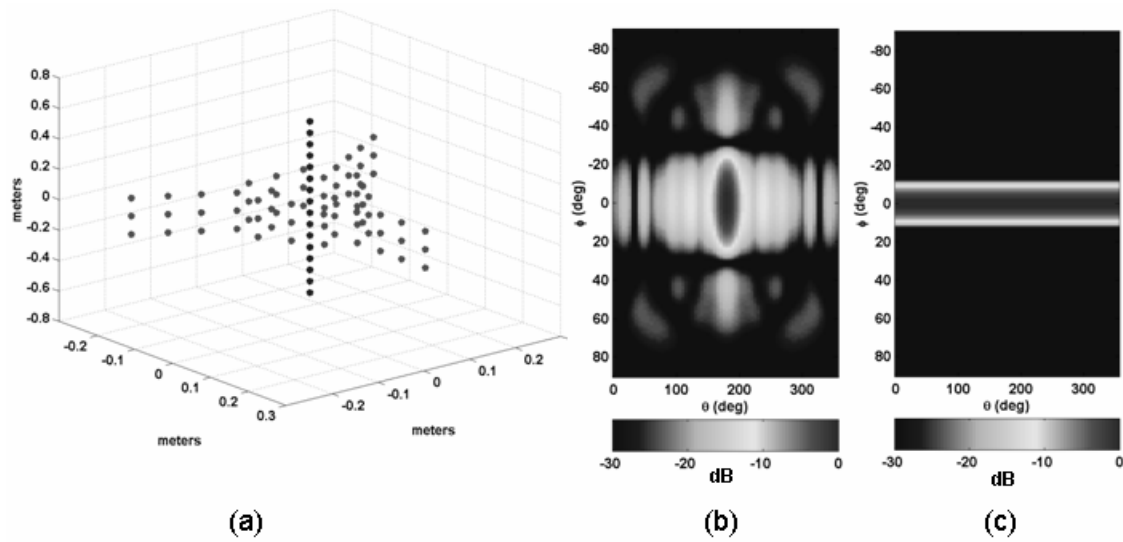


FIGURE 3. (a) Element positions of VLA and volumetric arrays, 8 kHz beam pattern steered horizontally for the volumetric array (b) and VLA (c).

Unity spatial weights are used for the volumetric array and Chebychev (-30 dB sidelobes) for the VLA. The volumetric array ambient noise response at 8 kHz versus vertical steering angle (negative looks up) and one azimuth direction is shown in Figure 4, given the noise directivities shown in Figure 1. [The response of all azimuthally steered beams will be essentially identical; however slight variations are expected due to the azimuth-dependent beam patterns]. The left panel shows the response using the dipole directionality model, and the right panel shows the response using the Kennedy monopole directionality model. The solid lines represent conventional beamforming (CBF) output and the light dotted lines modeled adaptive beamforming (MABF) assuming unconstrained minimum variance distortionless rejection (MVDR).

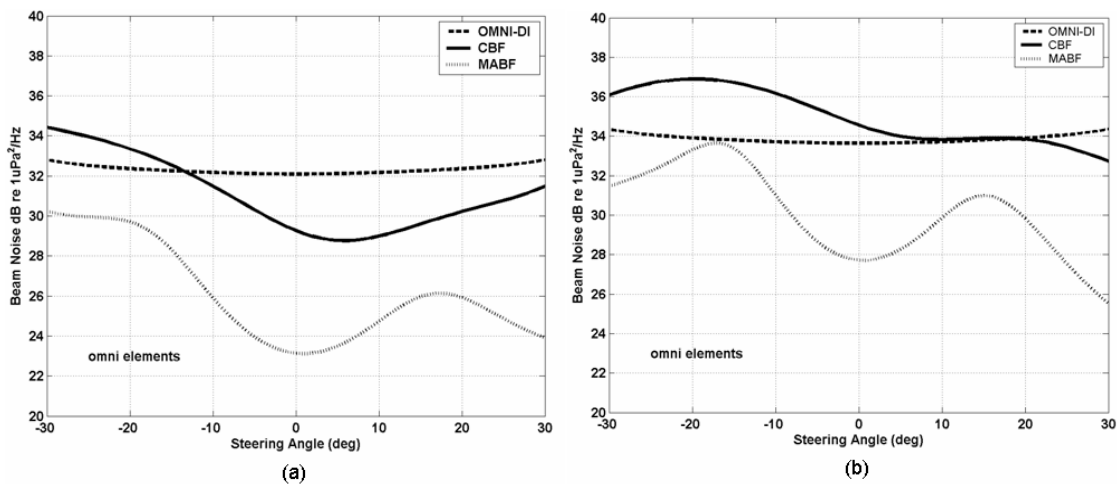


FIGURE 4. Ambient noise array response versus elevation angle at 8 kHz of the volumetric array assuming in the Straits of Hormuz summer (a) dipole source directionality and (b) Kennedy monopole source directionality.

The beam levels assuming isotropic noise are shown by the solid dashes in Fig. 4. The elevated response of the Kennedy model compared to the dipole model is expected based on the slight increase in omni level (Fig.1). Note the ability of adaptive methods to better resolve the ambient noise field structure in the notch region at the expense of possible poor white noise gain given the unconstrained adaptive processor. In recent work, not available at the time of writing of this paper, we have implemented a white noise gain constraint which provides robustness to uncorrelated noise passing through the beamformer.

Now consider that shipping noise generated via Eq. (9) is incoherently added to the CSD of the ambient. At 8 kHz, only ships near the receivers shown in Figure 2 are expected to generate sufficient noise to contaminate the ambient background. At 172°T, a tanker is located 4 km away, and a cluster of two tankers and one supertanker at ~270°T are located ~7 km away and another tanker is observed at ~0°T 17 km away. The response of the volumetric array (unity shading) to ships and ambient (Kennedy monopole source directionality model) at 8 kHz are shown in Fig. 5. The left panel shows the CBF response over all azimuthal steering directions (5° increments), as well as the level of the shipping omni level (44 dB). The right panel shows the result of MABF. Note the severe influence of the nearby ships on a significant number of azimuthal beams using CBF; considerable sidelobe leakage is apparent due to the poor sidelobe control in vertical and azimuth as shown in Fig. 3 (the remaining beams reach the ambient, similar to the solid curve in Fig. 4 (b)). This leakage is virtually eliminated using MABF; four distinctly elevated azimuthal beams are observed (individual ships), all other azimuthal beams reach the ambient levels, similar to the dashed curve in Fig. 4(b).

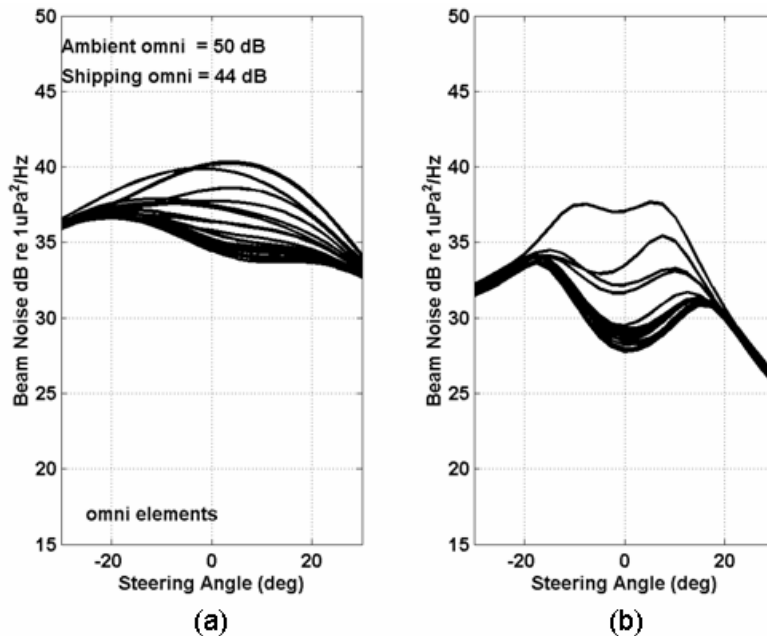


FIGURE 5. Ambient and shipping noise array response versus elevation angle at 8 kHz of the volumetric array assuming Kennedy monopole source directionality for ambient, (a) CBF processing and (b) MABF processing.

For sake of comparison, Figs. 6 and 7 show the response of the VLA in the same shipping field, using omni-directional and cardioid elements, respectively. For both cases, the Chebychev spatial window was used and the cardioid null was steered towards the nearest ship at 172° . The dashed curves show the response of the arrays to ambient alone.

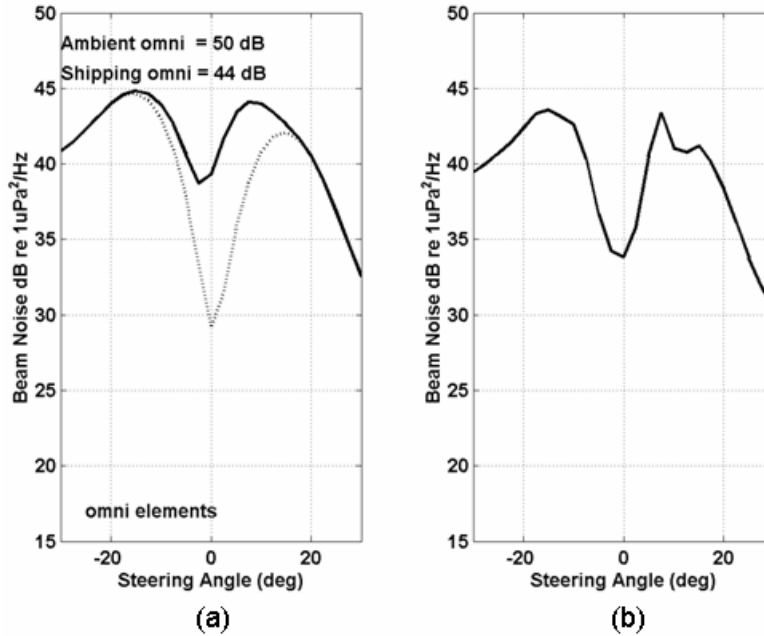


FIGURE 6. Ambient and shipping noise array response versus elevation angle at 8 kHz of the VLA (omni elements) assuming Kennedy monopole source directionality for ambient, (a) CBF processing and (b) MABF processing.

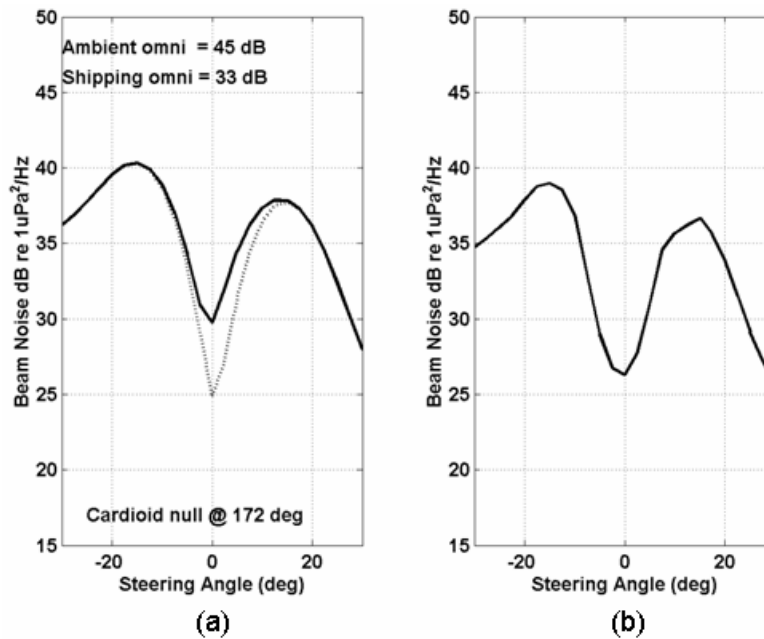


FIGURE 7. Ambient and shipping noise array response versus elevation angle at 8 kHz of the VLA (cardioid elements) assuming Kennedy source directionality for ambient, (a) CBF processing and (b) MABF processing.

Due to the low sidelobes provided by Chebychev shading, the 16 element VLA of omni elements is capable of theoretically measuring lower beam levels than the 72 element volumetric array in the notch with CBF, in the absence of shipping. But away from the notch, the beam levels rise rapidly. With shipping present, the notch gets filled in by 10 dB (Fig. 6(a)), although a shallow notch is still observed. The reason for this is that the VLA vertical beam width is narrow enough to steer into the ‘shipping noise notch’ and reject shipping noise in the vertical dimension. The volume scattering floor limits the level in this case. In the presence of shipping, MABF appears to provide 5 dB additional noise gain compared to CBF in the notch area. Note that the VLA has no ability to resolve ships in azimuth, hence there is only one curve shown. With the VLA of cardioids steered to null the nearest tanker at 172°T (Figure 7), the ambient level is reduced by 4.7 dB and the effective shipping level is reduced by 11 dB with CBF processing.

SUMMARY

A ray-based model has been developed to explore the sensitivities of wind-wave generated surface source directionality, volume scattering, element directionality and discrete shipping noise to the mid to high-frequency performance of a vertical line array and a volumetric array in a tactically relevant environment. Two surface source directionality models were shown in this paper to give different levels and structures to the ambient vertical noise directivity functions and corresponding array responses. Although based on empirical models found in the literature, future efforts by JHU/APL to develop physics-based surface directionality models will provide the necessary tools to validate the ambient noise model with measured data. In addition, the benefits of directional elements and adaptive methods were demonstrated to reduce the contamination of nearby ships in order to reach the ambient noise background.

ACKNOWLEDGEMENTS

The authors are grateful for the financial support from the IRAD program of the National Security Technology Department of the Johns Hopkins University / Applied Physics Laboratory.

REFERENCES

1. B. F. Cron and C. H. Sherman, "Spatial correlation functions for various noise models," *J. Acoust. Soc. Am.* **34** p. 1732 (1962)
2. W. S. Liggett and M. J. Jacobson, "Covariance of surface-generated noise in a deep ocean," *J. Acoust. Soc. Am.* **36** p. 303 (1965)
3. W. A. Kuperman and F. Ingenito, "Spatial correlation of surface generated noise in a stratified ocean," *J. Acoust. Soc. Am.* **67** p. 1988 (1980)
4. R. M. Hamson, "The theoretical responses of vertical and horizontal line arrays to wind induced noise in shallow water," *J. Acoust. Soc. Am.* **78** (5), p. 1702 (1985)
5. A.A. Aredov, N. N. Okhrimenko, and A.V. Furduev, "Anisotropy of the noise field in the ocean (experiment and calculations)," *Sov. Phys. Acoust.* **34** (2), p. 128 (1988)
6. R. M. Kennedy and T. K. Szlyk, "Modeling high-frequency vertical directional spectra," *J. Acoust. Soc. Am.* **89** (2), p. 673 (1991)
7. C. H. Harrison, "Formulas for ambient noise level and coherence," *J. Acoust. Soc. Am.* **99** (4), p. 2055 (1996)
8. C. H. Harrison, "Noise directionality for surface sources in range-dependent environments," *J. Acoust. Soc. Am.* **102**, p. 2655 (1997)
9. C. H. Harrison, R. Brind and A. Cowley, "Computation of noise directionality, coherence and array response in range dependent media with canary," *J. Comp. Acoust.* **9** (2), p. 327 (2001)
10. M. J. Buckingham and N. M. Carbone, "Source depth and the spatial coherence of ambient noise in the ocean," *J. Acoust. Soc. Am.* **102** (5), p. 2637 (1997)
11. G. B. Deane, M. J. Buckingham, and C. T. Tindle, "Vertical coherence of ambient noise in shallow water overlaying a fluid seabed," *J. Acoust. Soc. Am.* **102** (6), p. 3413 (1997)
12. "APL-UW High-Frequency Ocean Environmental Acoustic Models Handbook," APL/UW Technical Report 9407, (1994)
13. "Oceanic and Atmospheric Master Library Summary", Naval Oceanographic Office, Systems Integration Division, Stennis Space Center, MS 39522-5001, October 2002.
14. "Acoustic source levels of commercial vessels for use in sonar system modeling and analysis", Naval Undersea Systems Center, Tech. Memo 901157, August 1990.